Journal of the Korean Nuclear Society
Volume 30, Number 6, pp.485~495, December 1998

Effects of Aperture Density Distribution on the Flow Through a Rock Fracture with Line-Source and Line-Collection

Chung-Kyun Park and Pil-Soo Hahn
Korea Atomic Energy Research Institute
150 Dukjin-dong, Yusong-gu, Taejon 305-353, Korea

(Received February 10, 1997)

Abstract

Migration characteristics of tracers in a rock fracture in a case of line-source and line-collection was studied. The fracture plane was discretized into a square mesh to which variable apertures were assigned. The spatially varying apertures of a fracture were generated using a geostatistical method, based on a given aperture probability density distribution and a specified spatial correlation length. The flow potential and pressure at each node were computed. Calculations showed that fluid flow occurs predominantly through a few preferred paths. Hence, the large range of apertures in the fracture gives rise to flow channeling. The solute transport was calculated using a particle tracking method. The migration plumes of tracer between injection line and withdrawal line are displayed in contour plots. The elution curves are shown to be controlled by the aperture density distribution and to be insensitive to statistical realization and spatial correlation length.

I. Introduction

From the point of view of flow and transport, a fracture may be described by a prospective flow path with a variable fracture aperture formed between the fracture surfaces. Since the fracture surfaces are rough and undulated, the aperture widths are spatially varying. The wide range of aperture values in a single fracture gives rise to a very heterogeneous system and flow may be concentrated in a few preferred paths of least flow resistance. Thus, recent theoretical works[1,2] have taken into account that the aperture in a real rock fracture takes various range of values. Flow calculations on fractures with rough surfaces have been performed previously by some researchers [1,3]. Brown et al.[4] calculated fluid flow through a fracture constructed from a pair of rough surfaces placed at various separations. Each surface is independently generated from a fractal model of surface topography. They aimed to make a quantitative study of the deviation of flow through the constructed rough fracture from that based on the parallel plate idealization of the

Key Words : rock fracture, aperture, migration plume, particle tracking, channeling flow, solute transport

fracture. Tsang et al.[5] proposed a variable aperture channel model for transport through fractured media. While, Moreno et al[6] studied on the tracer transport between a line of injection point and a line of observation point, and examined channeling characteristics of flow through a natural rock fracture with the variable aperture channel model. They considered only for an advective flow as a solute transport mechanism and calculated for some limited cases.

As a serial work of Park et al.[2,7,8]' s study, we are going to develop a generalized model describing the migration of solutes in a rock fracture and to enhance the previous model such as Moreno et al[6]' s. In addition, we are to describe migration plume and pressure distribution in the fracture plane. Park et al.[7] studied contaminant transport through a rough-surfaced fracture in the case of point-source and point-collection already. The conclusion was that the correlation length of aperture distribution function was the most important parameter in that system. In this srtudy, we will describe a line collection and a line collection system. Comparing flow characteristics between two different systems is also one of the objectives of this study.

2. Transport Modeling

2.1. Fracture Aperture Generation

The variation of the fracture aperture in the fracture plane is characterized by a spatial correlation length. This means that for distances in the fracture plane smaller than the correlation length the aperture widths are more likely to be similar, but at distances larger than the correlation length there is little or no correlation among apertures at different locations.

To calculate the fluid flow and solute transport through a single fracture with variable apertures, the fracture plane is partitioned by grids with different apertures assigned to each square enclosed by grid lines. For most of the present study, the number of squares are 20×20. The assignment of the apertures is by means of a geostatistical method which generates a two-dimensional field of a correlated distributed parameter.

For the purpose of the present study we chose a log-normal distribution for the variable apertures in the plane of the fracture and an exponential function for the spatial covariance of the apertures to assign different aperture values for the divided individual square mesh[9]. We introduce the martix decomposition method[10] to generate the log-normally distributed values of fracture apertures b which are first transformed to the normal distribution Y

$$Y = log_{10}\, b \tag{1}$$

The values of Y are estimated from

$$Y = M \cdot \epsilon + \nu \tag{2}$$

in which ν is the mean of Y, ϵ is a normally distributed vector N [0,1] with mean of 0 and standard deviation of 1 , and M is defined in terms of the covariant matrix

$$A = MM^T \tag{3}$$

Eq. (2) represents the generated process because the mean is given by

$$E[Y] = M\, E[\epsilon] + \nu = \nu \tag{4}$$

in which E stands for the expected value and the covariance is given by

$$E[(Y-\nu)(Y-\nu)^T] = M\, E[\epsilon\epsilon^T]\, M^T = MM^T = A \tag{5}$$

We used the exponential form of the covariance function

$$A = \sigma^2 \exp(-\alpha r) \tag{6}$$

in which σ^2 is the variance of Y, r is the separation lag, and α is the autocorrelation parameter which has the dimension of inverse length. The exponential form of Eq.(6) indicates that quantities within a distance on the order of $2/\alpha$ will be correlated and thus we may define the correlation length, λ, to be $2/\alpha$. The form of Eq.(6) indicates that the covariance chosen is isotropic.

The generation scheme is performed as follows. First, the covariance matrix A is formed by using Eq.(6) for a set of different locations. Second, the matrix M is estimated using the Choleski decomposition technique. Third, the vector ε is calculated by generating random numbers with an intrinsic FORTRAN subroutine[9]. Hence, a different starting number or seed (R_o) gives a different set of vector ε. Fourth, the vector Y is estimated from Eq.(2).

Fig.1 shows the realization of statistically generated aperture field in the case of the mean of the lognormal aperture density distribution ν=1.0, the standard deviation of the distribution σ=0.6, and the correlation length λ=0.5. The upper part in Fig.1 is a contour plot of aperture distribution in the fracture plane and numeric data in the contour map show values of apertures in the unit of *cm*. The lower part in Fig.1 is a surface plot of the same aperture distribution, where y axis is magnified. It shows that relatively low aperture value consists the major portion of the aperture population,

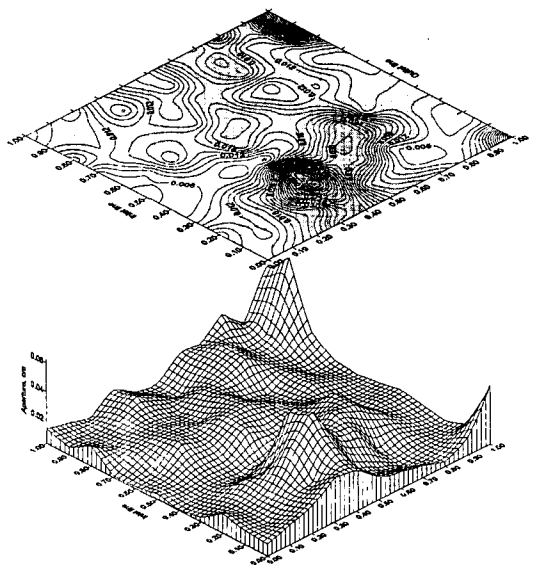

Fig. 1. The Aperture Density Distribution over the Two-dimensional Fracture and Topographic Map

2.2. Flow Field in the Rock Fracture

The fluid flow through the fracture was then calculated for a constant injection/withdrawal rate as well as for constant pressure conditions. For a constant laminar flow, the volumetric flow rate through a parallel fracture may be written as:

$$Q = \frac{1}{12\,\mu}\,\frac{b^3\,W}{L}\,\Delta P \tag{7}$$

where ΔP is the pressure drop over a length of L and W and μ is the viscosity. Eq. (7) may be applied to each of the subsquares enclosed by grid lines. When the volumetric flow rate from node i to node j is denoted by Q_{ij}, the pressure drop from node i to node j can be written,

$$\begin{aligned}\Delta P = P_i - P_j &= \frac{Q_{ij}}{\frac{2\,b_i^3\,\Delta y}{12\,\mu\,\Delta x}} + \frac{Q_{ij}}{\frac{2\,b_j^3\,\Delta y}{12\,\mu\,\Delta x}} \\ &= Q_{ij}\left[6\mu\,\frac{\Delta x}{\Delta y}\left(\frac{1}{b_i^3}+\frac{1}{b_j^3}\right)\right]\end{aligned} \tag{8}$$

where P_i is the pressure at node i, and Δx and Δy are the length of x and y coordinate of the subsquare, respectively. Node i implies an index of the ith subsquare in the fracture surface. Then the

volumetric flow rate can be rewritten as,

$$Q_{ij} = C_{ij}(P_i - P_j) \tag{9}$$

where C_{ij} is the flow conductance between nodes i and j.

$$C_{ij} = \frac{1}{6\mu}\frac{\Delta y}{\Delta x}\left(\frac{1}{b_i^3}+\frac{1}{b_j^3}\right)^{-1} \tag{10}$$

The mass balance at each node may be written as:

$$\sum_j Q_{ij} = \sum_j C_{ij}(P_i - P_j) = E_i \tag{11}$$

where E_i is the injection rate or withdrawal rate at node i. The j stands for the four facing nodes to node i. Except for the nodes at the boundaries, the pressure at each node can be solved with the Gauss-Seidel method. The flow between adjacent nodes can be calculated using Eq. (9).

The simulated pressure field is shown in Fig. 2. The numerical values in upper part of Fig. 2 are the pressure distribution in N/m^2. The pressure drop between the injection and withdrawal faces are about 250 N/m^2. The withdrawal line is near atmospheric pressure and the pressure at the injection line is calculated to be 101586.9 N/m^2.

The volumetric flow rates at each node are plotted as vector distribution in Fig. 3, where for display purposes the size of the arrow is proportional to the flow rate. The flow rates between the nodes vary over several orders of magnitude. The large range of values is arised from the fact that the local resistance to the flow is inversely proportional to the local aperture by the third power, and the lognormal distribution of apertures originally assumed for the fracture plane gives rise to a wide range of values. The plot in Fig. 3 correspond to the pressure distribution of Fig.2a for a given aperture variations shown in Fig. 2b. This figure displays the preferred paths of

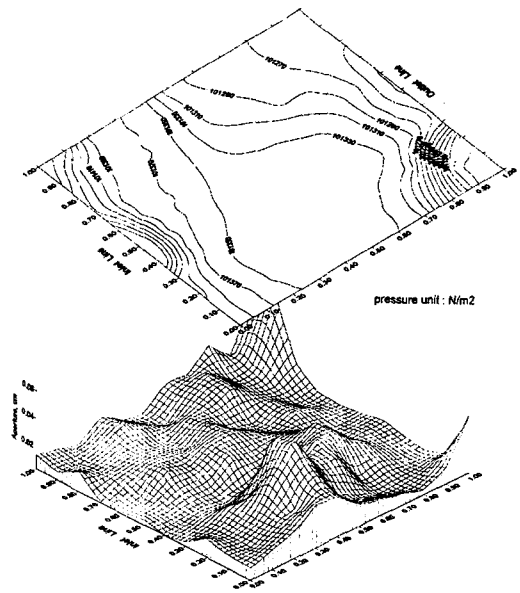

Fig. 2. Topographic Map of Pressure Distribution in the Fracture

large volumetric flow that are formed because of the variation of the apertures within the fracture as already mentioned. While, even though the portion of the large aperture is of little, the effect on the resulting flow can be dominant. That is, the major portion of groundwater will flow through the small portion of the larger aperture path.

2.3. Particle Tracking Method for Solute Transport

Solute transport phenomena are investigated by tracking the particle advected through the fracture. Recall that the boundary conditions employed to solve the flow through the system are the constant head boundary condition; that is, all the nodes on the left-hand boundary in Fig. 3 are connected at the higher pressure, and all the nodes on the right boundary are connected at the lower pressure. Particles are let in at the left-hand boundary and collected at the right-hand boundary. The particles are distributed in proportion to the flow rates at

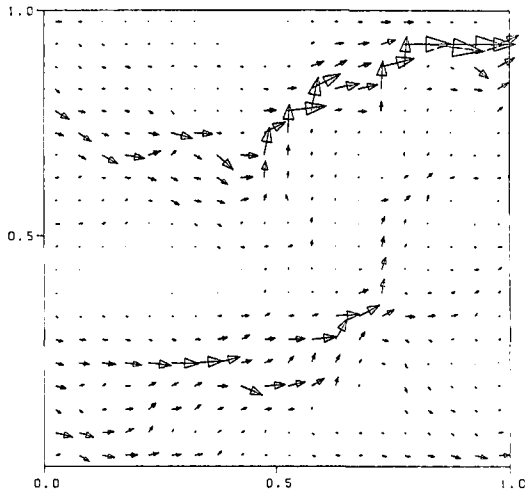

Fig. 3. Flow Vector Distribution in the Fracture Plane the Size of the Arrow is Proportional to the Flow Rate

different nodes along the inlet boundary.

A particle, which is representing the mass of a solute contained in a defined volume of groundwater, moves through a fracture with two types of motion. One motion is with the mean flow along stream lines and the other is random motion, governed by scaled probability. Particles are then convected by discrete steps from node to node until they reach the outlet node at which point the arrival time is recorded. The residence time of a particle along each path is obtained as the sum of the residence times in all subsquares through which the particle has passed. Four transport processes are considered in modeling : advection, longitudinal dispersion, diffusion into the rock matrix, and sorption[11]. Calculations have been carried out for a total number of input particles ranging from several hundreds to 10,000 in order to investigate the effect of the number of particles on the elution curves. Calculations using 2000 particles are more than adequate since they already yield stable curves that have few spurious artifacts due to the finite number of particles employed. 10,000 particles are used in this simulation.

4. Migration Plume and Channeling Flow

Fig.4 shows the spatial distribution of particles for test no.1 at times from 10 min. to 40 min. after injection. It is a contour plot of the number of particles in the fracture. The number of particles at each node is normalized by dividing by the total number of particles injected. Numerical values in the contour maps are the normalized concentration, *C/Co*, in which *Co* is the initial input concentration. Not only are we interested in the total elution of tracer transport, but we are particularly interested in the manifestation of the channeling phenomenon in the tracer measurements. These plots show that the solute moves as a broad lump rather than moving a straight line from the inlet to the outlet. Comparing to the aperture and pressure distributions as shown in Fig.2, the migration plume displays the prefered path of large flow rate that is formed by the variation of the apertures. In other words, the flow through the fracture follows the least resistive pathways composed of largest apertures. Channeling flow implies that some fast pathways might transport a portion of the nuclides considerably faster than the average. The flow through smaller apertures will be little because the local resistance is inversely proportional to the cube of local aperture in Eq.(7).

A plot of the number of particles collected at all the outlets on the right-hand boundary at different arrival times constitutes the elution curve as shown in Fig.5. The elution curves involve the residence times of all flow paths which originate from the injection line and terminate at the exit line. Here t_m can be calculated by two ways. Firstly, tm is calculated by taking the average residence time of the all particles injected. Secondly, it can also be

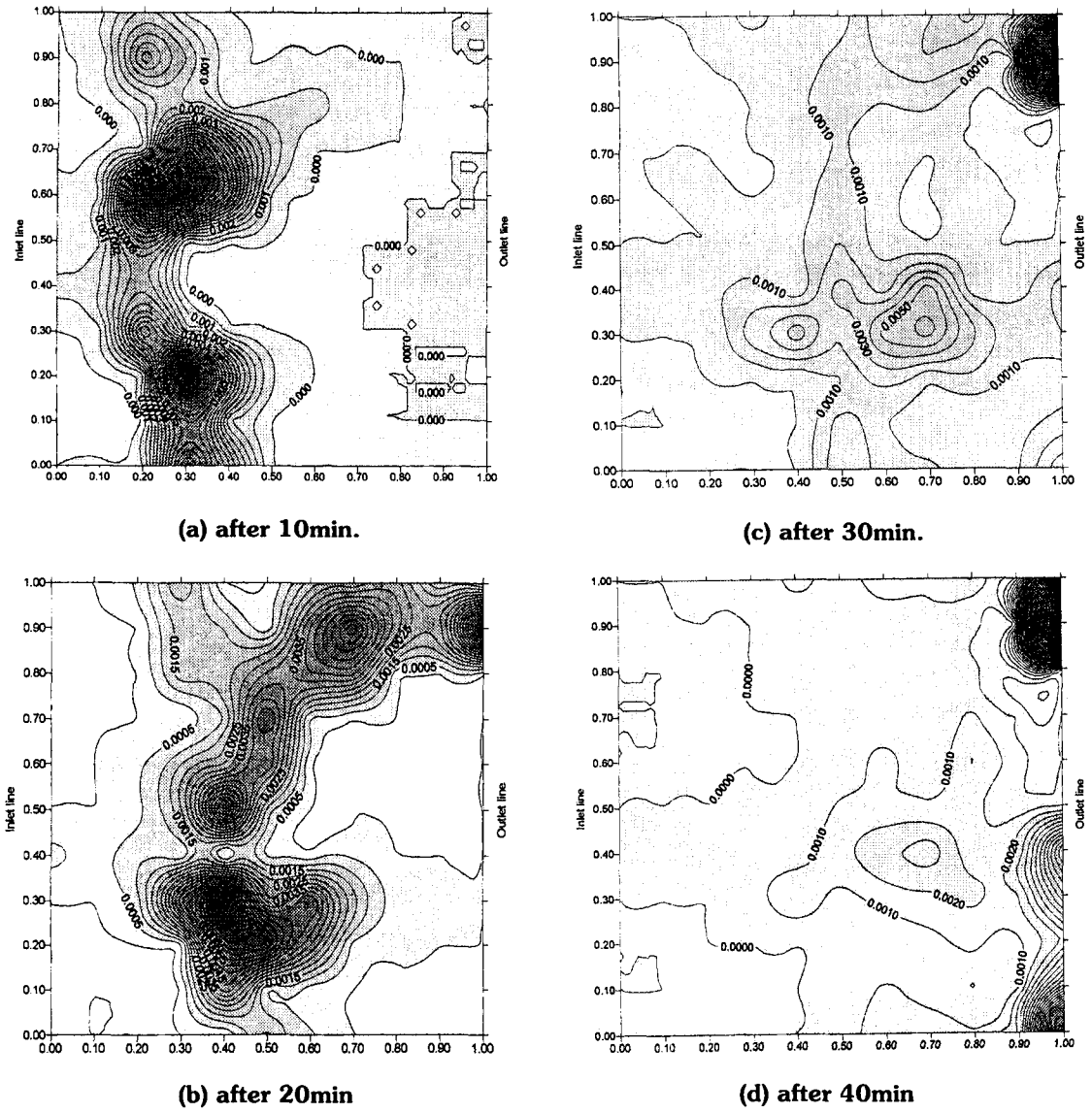

Fig. 4. Contours of Migration Plume with Time in the Fracture

calculated from the main peak of the elution curves when a pulse function is injected. The t_m in Table 1 is estimated by this second method. If there is no long tail, two methods are reasonably agreed with each other.

A sharp rise of the elution curves at early stage can be interpreted that the majority of particles take the fast flow paths, then there is a long tail in the elution curve due to a small fraction of particle meandering within the fracture.

5. Parameter Sensitivity Studies

We have discussed the general behavior of flow and transport through a fracture with variable apertures governed by a particular set of aperture parameters. We now turn to study the effect of the variation of these aperture parameters on the flow and transport. The parameter sensitivity study was carried out by varying (1) the standard deviation in the lognormal aperture density distribution, (2) the spatial correlation length of the apertures, and (3) the flow path, more specifically, the different realization of the fracture field.

The transport properties for the different conditions are studied by comparing the mean residence time and dispersion. The mean residence time and variance may be used to determine the Peclet number, P_e [12], which is a dimensionless measure of the dispersivity

$$\frac{2}{Pe} = \frac{\sigma_t^2}{t_m^2} \tag{12}$$

where

$$t_m = \frac{\int_0^\infty tCdt}{\int_0^\infty Cdt} \tag{13}$$

is the mean residence time and $C(t)$ is the tracer concentration at a given time, t. The second moment as a measure of hydrodynamic dispersivity is

$$\sigma_t^2 = \frac{\int_0^\infty (t-t_m^2)Cdt}{\int_0^\infty Cdt} \tag{14}$$

On the other hand, in the case of high dispersion, t_m is strongly influenced by the tail of the elution curve as mentioned in section 5 and the determination of P_e with Eq. (13) yields value that is also dominated by the tail. An alternative method for estimating P_e from the elution curves is to make use of the arrival time for C/Co = 0.1, 0.5, and 0.9 [11]. This method emphasizes the dispersion up to C/Co = 0.9 and de-emphasizes the role of the tail. From the arrival time, the ratio, $t_R = (t_{0.9}-t_{0.1})/t_{0.5}$ is determined and P_e calculated from a curve of P_e versus t_R obtained from the solution of the advection-diffusion equation for a porous medium [14]. The breakthrough curve can also be obtained by integrating the elution curve for step input function. This method does not take into account the part of the curve below 10% and above 90%. P_e calculated using this relationship is usually larger than that calculated by means of moments from Eqs.(12) and (14).

Throughout the sensitivity study, the mean aperture is maintained constant by requiring the aperture parameter to obey the distribution function. Fractures with variable apertures were generated with a specified set of aperture parameters (σ, λ, R_o) using the method described in section 2.2, then simulations for flow and transport were carried out. Seven realizations of fracture apertures corresponding to each set of parameters were generated in order to study the dependence of results on the realization. The flow properties chosen as criteria to compare the different cases are the residence time in the fracture, t_m, and the Peclet number, P_e. The parametric values and results are shown in Figs. 5, 6, & 7.

5.1. Dependence on Flow Path

Set 1 deals with three realizations of statistically generated apertures with the identical lognormal aperture density distribution but with different flow paths, which are generated by introducing different random number seeds(R_o). The values of parameters used are arranged in Table 1. The overall morphology of surface and flow path are changed from realization to realization. Thus the

Table 1. Parameter Values and Simulation Results

Set No.	Test No.	ν	R_o^*	σ	λ	t_m	P_e
Set 1 :	1	1	#1	0.6	0.5	28	6.5
Flow Path variation	6	1	#2	0.6	0.5	48	8.0
	7	1	#3	0.6	0.5	50	8.5
Set 2 :	4	1	#1	0.1	0.5	20	48
σ variation	5	1	#1	0.3	0.5	23	30
	1	1	#1	0.6	0.5	28	6.5
Set 3 :	2	1	#1	0.6	0.1	26	5.0
λ variation	3	1	#1	0.6	0.25	22	6.0
	1	1	#1	0.6	0.5	28	6.5

R_o^* : Seed index No. for generating random numbers.

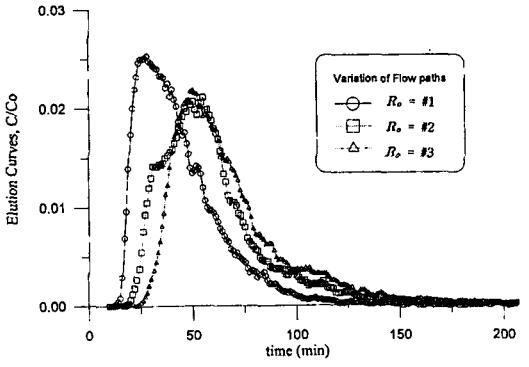

Fig. 5. Elution Curves for Various Flow Paths

elution curves may also be changed according to the change of flow paths. The results of simulation are shown in Fig. 5. In this figure and Table 1, the values of t_m and P_e do not change significantly comparing to the other parameter sets. Therefore, when the geostatistical relationship is maintained in each realization, the overall flow resistance does not change significantly and elution curves also show a similar trend.

5.2. Dependence on Aperture Variance

Set 2 deals with the effect of aperture variation while the correlation length and the mean of aperture are kept constant. Also the overall morphology of surface and flow path are schemed to be roughly maintained with σ variation while the aperture and the flow resistance are changed at each point in the fracture. Fig.6 shows the elution curves for these σ values. P_e is about 6.5 for σ of 0.6. When the σ is 0.1, then P_e is about 48. This shows the strong influence of the width of the fracture aperture distribution on the dispersion of tracers flowing through it. In this system, the dispersion is mainly due to the channeling effects as shown in migration plume. This means that for a very small σ, the dispersion is negligible. In the limit when σ is 0, the dispersion is zero, that is, plug flow in a constant aperture parallel plate fracture. These trends may be explained by the fact that a larger σ means a greater number of small apertures. The small apertures strongly reduce the flow in these locations. On the other hand, the flow is mainly concentrated on fracture with large apertures if they are not isolated. Otherwise, they may increase the residence time in the fracture but not the flow rate in it. However, if these large apertures are connected from one side of the fracture to the other, larger flow may be observed. Fig.6 and P_e values in Table 1 show that the most

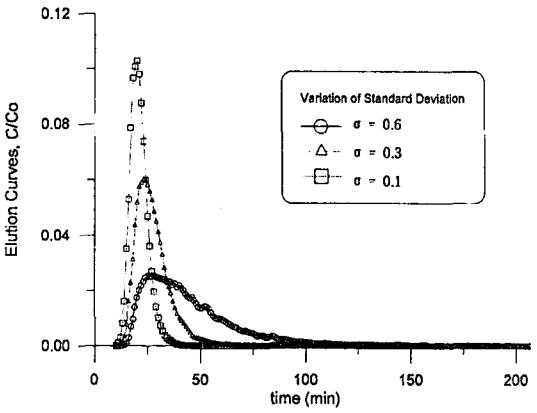

Fig. 6. Elution Curves for Various Values of the Standard Deviation

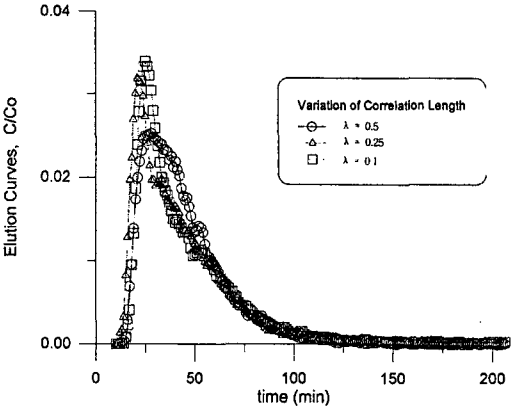

Fig. 7. Elution Curves for Various Values of the Correlation Length

important parameter affecting the flow properties is σ. The dispersion of the solute transport is increased as σ increases.

5.3. Dependence on Corrreation Length

Set 3 deals with the effect of correlation length. As the case of σ variation, the overall morphology of surface and flowpaths are schemed to be roughly maintained with variation even though the value of aperture and the flow conductance are changed at each node in the fracture. The results are shown in Fig.7 and Table 1, and they show that the hydrodynamic properties (t_m, P_e) are slightly sensitive to the different values of λ. When λ is increased from 0.1 to 0.5, the dispersion of the tracer is slightly reduced, i.e., P_e is slightly increased. By the way, Moreno et al.[6] obtained an opposite result in the same kind of line-injection and line collection system, that is, when λ is increased, σ^2_t is increased and P_e is decreased. However, the flow property of the system λ is insensitive to the λ variation in both systems. The range of λ values from 0.1 to 0.5 implies that λ is of the same order of magnitude as the flow length, which is appropriate when the channeling phenomenon is occured. These elution curves involve the residence times of all flow paths which originate from the injection line on the left boundary and terminate at the exit line on the right boundary, both boundaries cover several spatial correlation lengths. So the information contained in the elution curves is an average over several correlation lengths, hence the hydrodynamic properties are insensitive to λ. While test involving point injection and point collection is influenced by the local heterogeneities of the system, thus the hydrodynamic properties may fluctuate very much depending on the positions of the injection and collection [9].

From the results of numerical simulation with Sets 1 through 3, the most important parameter to affect the flow and solute transport is σ, the standard deviation in the lognormal aperture distribution. If σ is increased, the flow in the fracture is decreased and the dispersion increased. This conclusion is, however, specific for the present case, where both injection and collection are along lines of fracture. It does not apply to the cases with point injection or point observation of tracers [9]. In that case, the most sensitive parameter is the correlation length, λ.

6. Conclusions

For the calculation of flow and tracer transport in a rock fracture, a variable aperture channel model is introduced successfully. Matrix decomposition method can be applied in describing variable aperture fields. Calculated results are shown in the form of elution curves and migration plumes. These are correlated with the basic input parameters of aperture density distribution function. Simulated migration plumes and elution curves show that a broad distribution of apertures in the fracture results the channeling flow. The channeling phenomena mean some fast pathways that might transport the majority of the solute while a small portion of solutes meandering through the fracture gives rise to a long tail. Results of the parameter sensitivity studies show that the most important parameter which affects the flow and tracer transport is the standard deviation of the aperture in the fracture. If the parameter is increased, a larger number of small apertures results in the increase of the flow residence time and consequently the enhanced hydrodynamic dispersion.

Nomenclature

b fracture aperture in cm

C_{ij} flow conductance between nodes i and j in $cm^4\ s/g$

E_i injection rate or withdrawal rate at node i in cm^3/s

g gravitational acceleration in cm/sec^2

μ viscosity of the transport solution in $g/cm.sec$

r density of the transport solution in g/cm^3

P_i pressure at node i in $dynes/cm^2$

p_{ij} probability of the flow from node i to node j

Q_{ij} volumetric flow rate from node i to node j in cm^3/s

t_i residence time of a particle in node i

t_m mean residence times of the particles at exit

t_{cum} cummulative travel time of a particle along the flow path

σ^2 variance of the aperture density distribution

σ^2_t variance of the elution curves

References

1. Neretnieks.I., T. Eriksen, and P. Tahtinen. "Tracer movement in a single fissure in granitic rock : Some experimental results and their interpretation," *Water Resour. Res.*, **18**(4), 849-858, (1982).
2. Park,C.K., Hahn, P.S. "Interpretation of Migration of Radionuclides in a Rock Fracture Using a Particle Tracking Method," *J. of Korean Nucl. Soc.*, **27** (2) , 176 (1995).
3. Patir, N., and H.S.Cheng, "An average flow model for determining effects of three-dimensional roughness in partial hydrodynamic lubrication," J. Lubr. Rechnol., 100, 12-17, (1978).
4. Brown, S.R., "Fluid flow through rock joints: The effect of surface roughness," *J. Geophys. Res.*, **92**(B2), 1337-1347, (1987).
5. Y.W. Tsang, C.F.Tsang, I.Neretnieks and L.Moreno, "Flow and tracer transport in fracture media- A variable-aperture channel model and its properties," *Water Resour. Res.*, **24**(12), (1988).
6. L. Moreno, Tsang C.F., Hale, F.V. and Neretnieks, I. "Flow and tracer transport in asingle fracture," *Water Res. Res.* **24**, 2033, (1988).
7. Park,C.K., Keum,D.K. and Hahn, P.S., "Stochastic Analysis of Contaminant Transport through a Rough-Surfaced Fracture," *Korean J. of Chem.Eng*, **12** (4), 428, (1995).
8. Park,C.K., Hahn, P.S.,and T. T. Vandergraaf, "Analysis of the Migration of radionuclidess in a natural fracture in granite using a variable

Aperture Channel Model," *J. of Contaminant Hydrology*, **17** (1997).

9. Mantoglou,A. and Wilson,L., "The turning bands method for simulation of random fields using line generation by a spectral method," *Water Resour. Res.*, **18**(5), 1379-1394, (1982).
10. El-Kadi,A.I., *Model variability in groundwater flow*, International Groundwater Modeling Center, GWMI 84-10, Holcomb Research Institute, Butler Univ. (1984).
11. A.J. Desbarats, Macrodispersion in Sand-Shale Sequences, *Water Resour. Res.*, **26** (1), 153, (1990).
12. Levenspiel, O., *Chemical Reaction Engineering*, 2nd ed., John Wiley, New York, (1972).